

Fig. S1 Piezoelectric performances of electrospun mats loaded with different concentrations of ZnO. (A-C) Voltage and current output of electrospun fiber mats with zinc oxide at different loads (10 MΩ, 50 MΩ, and 100 MΩ). (D) The voltage output of electrospun mats of 1,2,4 and 8 wt% ZnO at loads of various resistances.

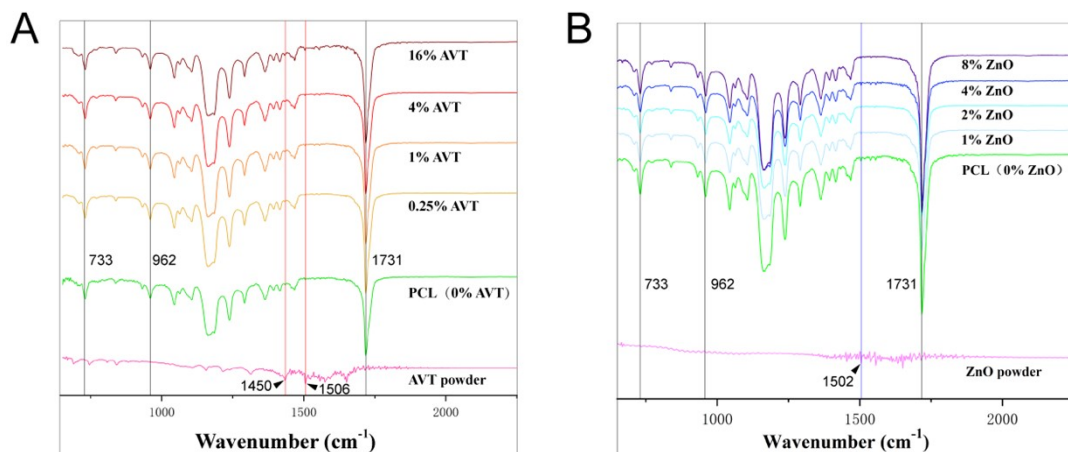


Fig. S2 FTIR examination of coaxial electrospun mat and ZnO and AVT powders. (A) FTIR for electrospun mats loaded with different concentrations of AVT and AVT powder. (B) FTIR for electrospun scaffolds loaded with different concentrations of ZnO and ZnO powder.

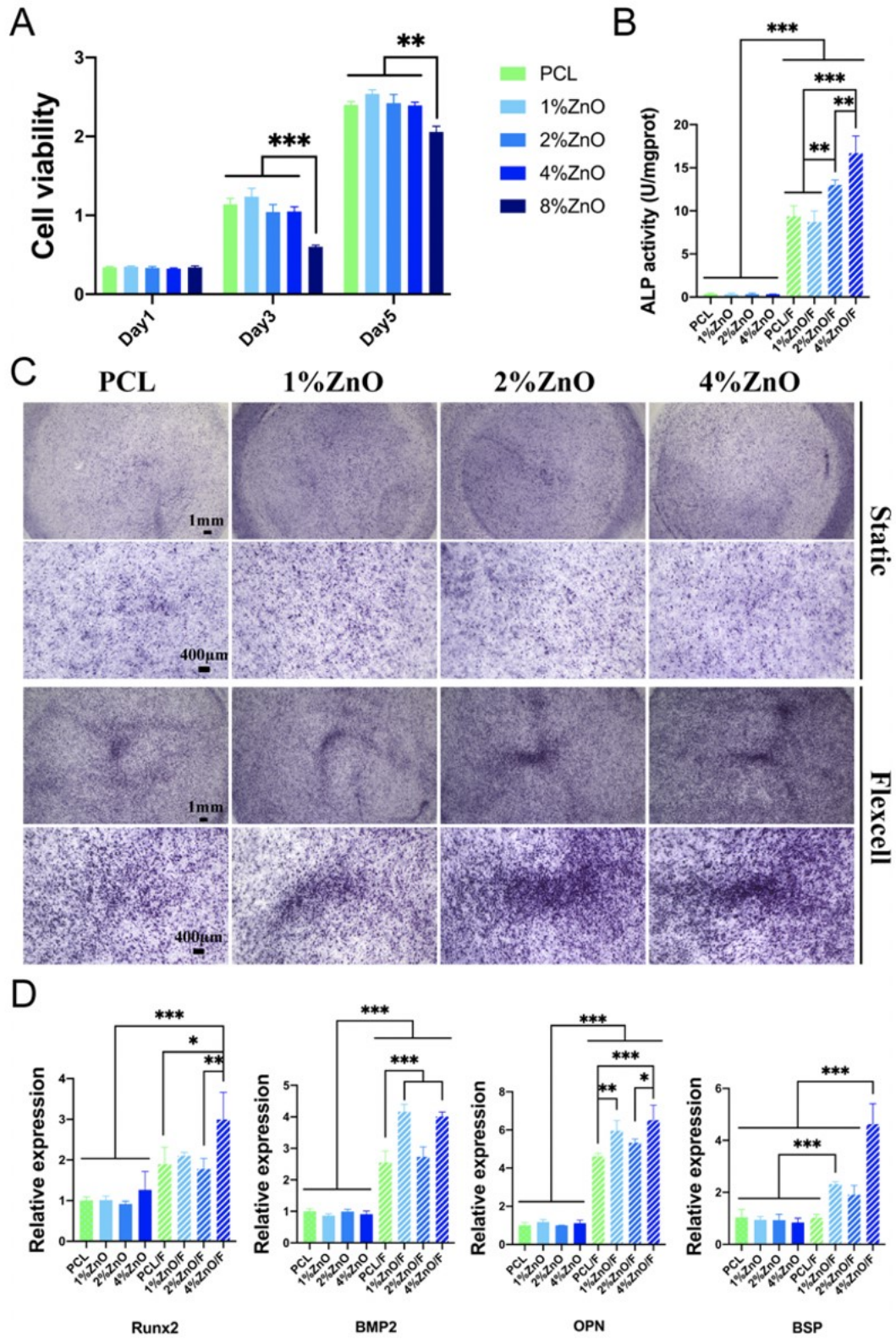


Fig. S3 Biocompatibility and osteogenic properties of electrospun mats. (A) Cell proliferation of BMSCs incubated on electrospun mats loaded with 0% ZnO, 1% ZnO,

2% ZnO, 4% ZnO, and 8% ZnO was examined on days 1, 3, and 5 by CCK-8 kit. (B) Quantification of ALP activity of BMSCs cultured on different ZnO electrospun mats at day 4 under static and dynamic environments. (C) Representative ALP staining images of BMSCs cultured on various ZnO mats after 7 days of incubation. (D) PCR assay for marker genes of osteogenesis differentiation (Runx2, BMP2, OPN, and BSP). /F indicates culture in the Flexcell system, i.e. dynamic culture environment. Data are expressed as mean \pm standard deviation (SD) (n=3). The significance of data was calculated by one-way ANOVA (*represents $p < 0.05$, **represents $p < 0.01$, ***represents $p < 0.001$).

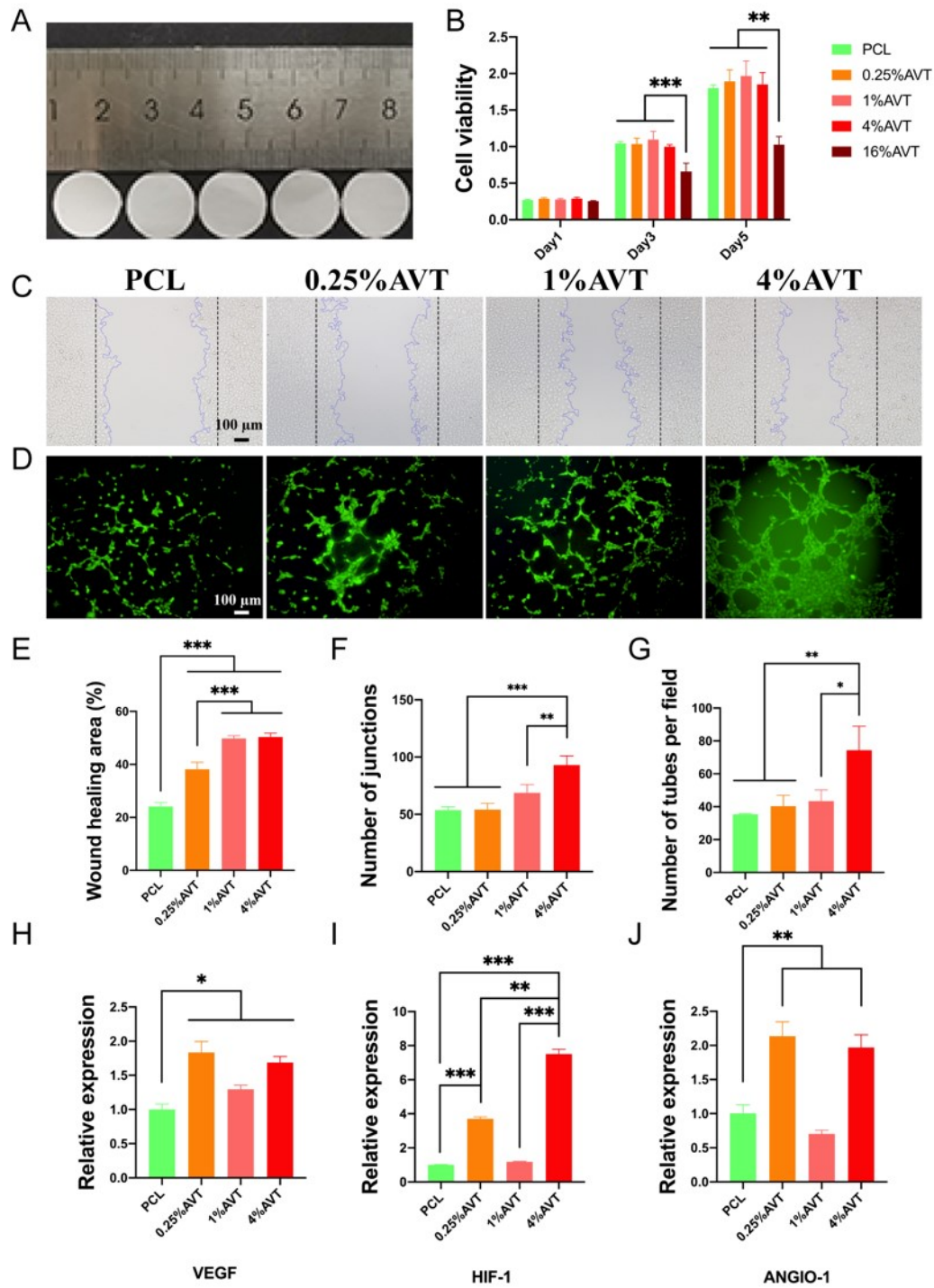


Fig. S4 Biocompatibility, cell migration, and angiogenic properties of HUVECs on electrospun mats. (A) Digital photographs of electrospun mats containing different concentrations of atorvastatin with a diameter of 14 mm. (B) Cell proliferation of HUVECs incubated on electrospun mats loaded with 0% AVT, 0.25% AVT, 1% AVT,

4% AVT, and 16% AVT was assessed on days 1, 3, and 5 using the CCK-8 kit. (C) Representative images of wound healing after 24 hours of culture. (D) Representative image of HUVEC tube formation after 4 hours of incubation on Matrigel. (E) Quantitative analysis of wound healing area. (F) The number of tubule connections in tubulation examination. (G) the number of mesh in the tubule formation assay. (H-J) PCR assay for marker genes of vascular differentiation (VEGF, HIF-1, and ANGIO-1). Data are expressed as mean \pm standard deviation (SD) (n=3). The significance of data was calculated by one-way ANOVA (*represents $p < 0.05$, **represents $p < 0.01$, ***represents $p < 0.001$).

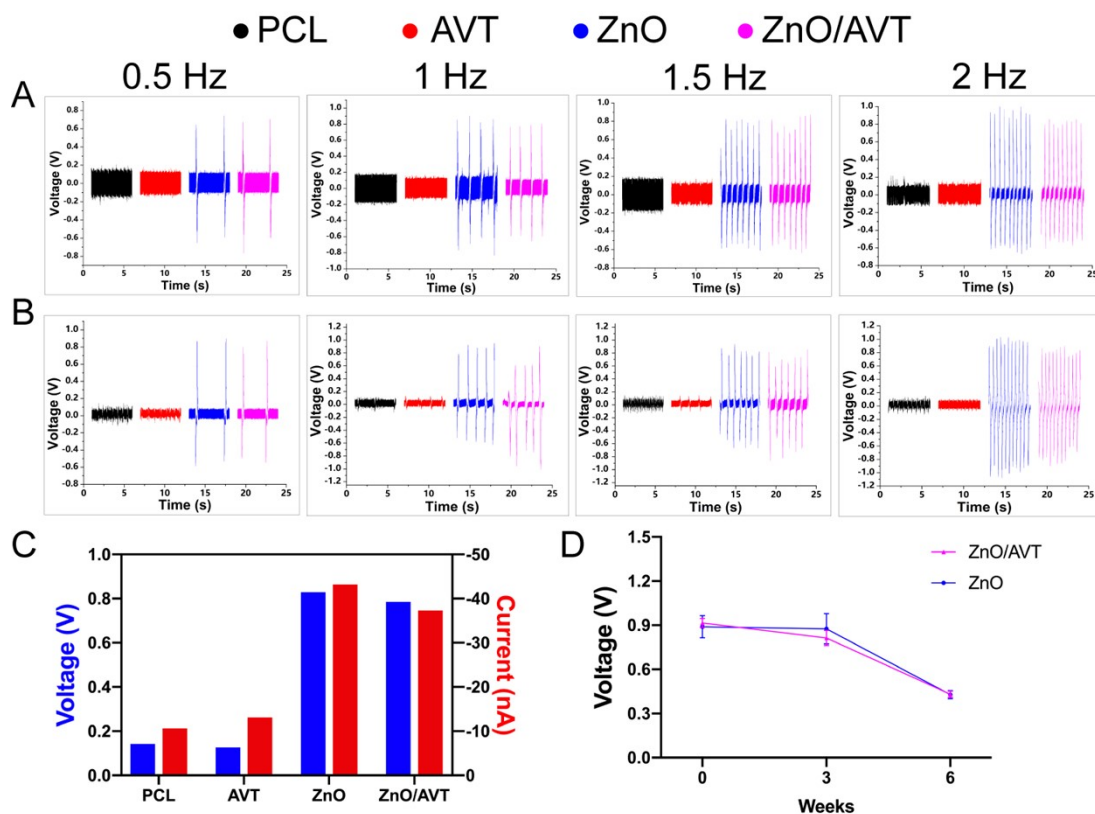


Fig. S5 Characterization of the electrical properties of electrospun fiber mats in vivo and in vitro. (A) Voltage output of PCL group, AVT group, ZnO group, and ZnO/AVT group under compression test at different frequencies. (B) Voltage output under bending test at different frequencies. (C) Voltage and current output of electrospun mats (a loaded of 100 M Ω). (D) Voltage output after 3 and 6 weeks of PBS immersion.

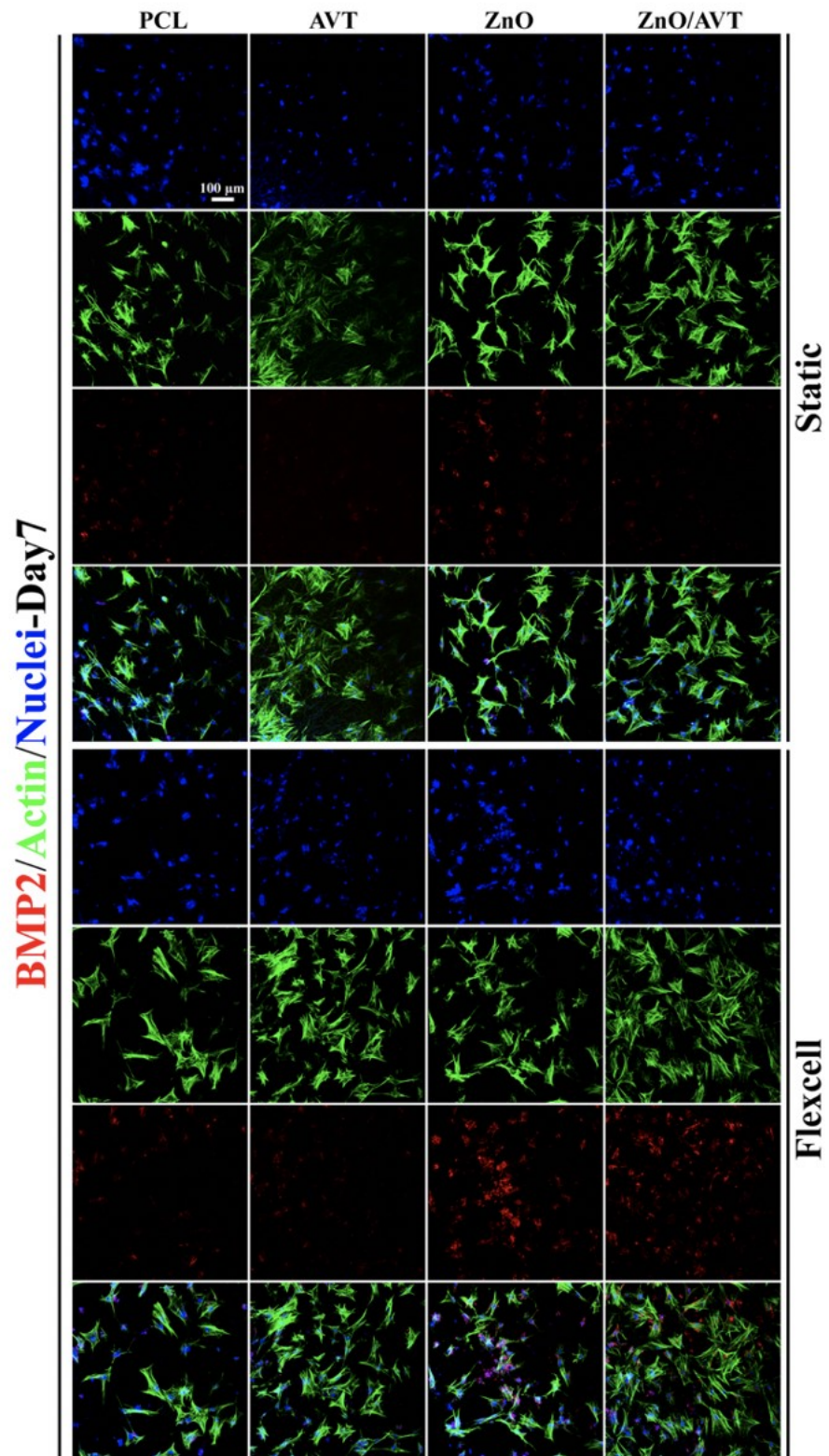


Fig. S6 Immunofluorescence staining of BMP2 in BMSCs after 7 days of culture on different mats.

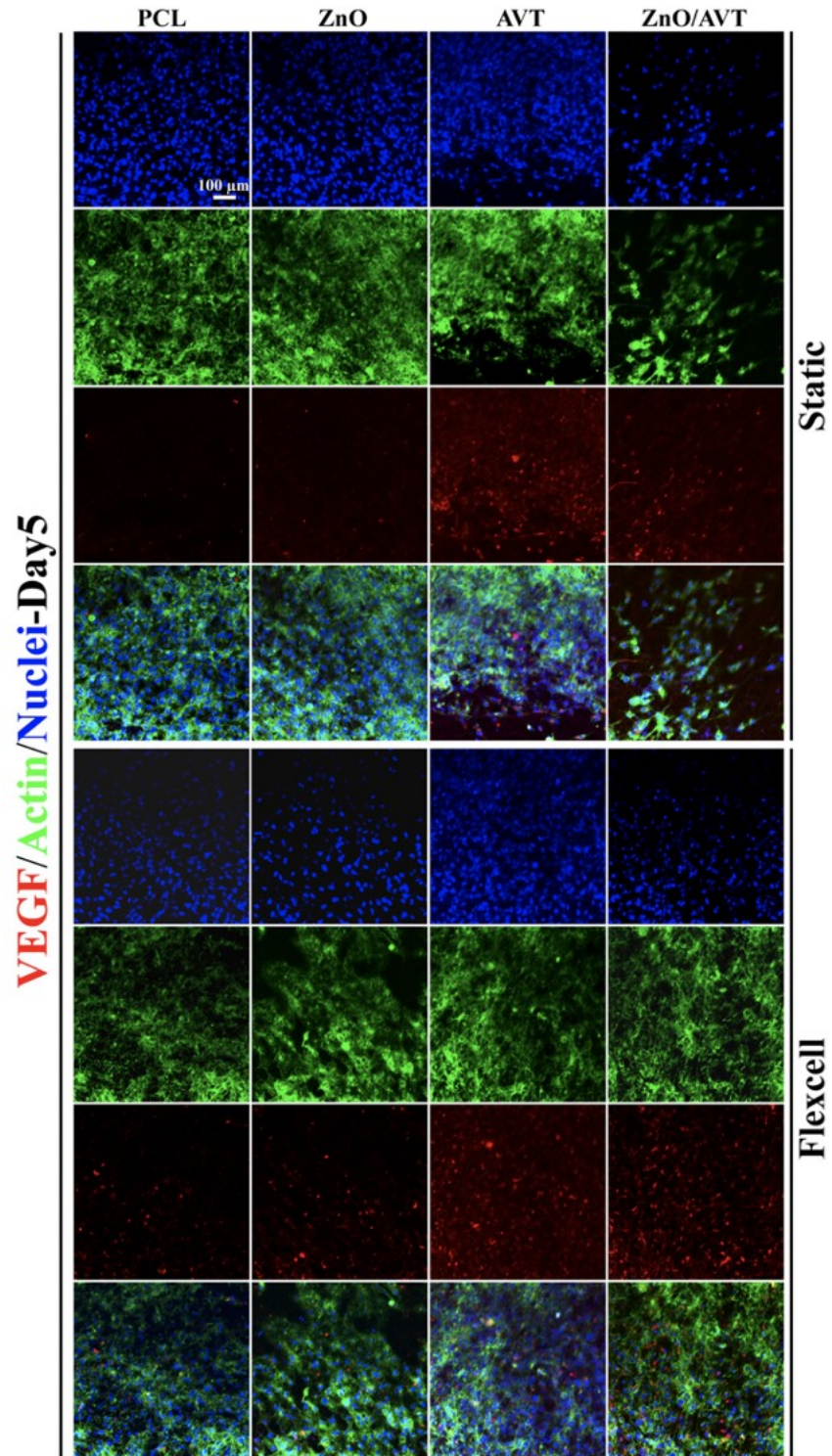


Fig. S7 Immunofluorescence staining of VEGF in HUVECs after 5 days of incubation on different mats.

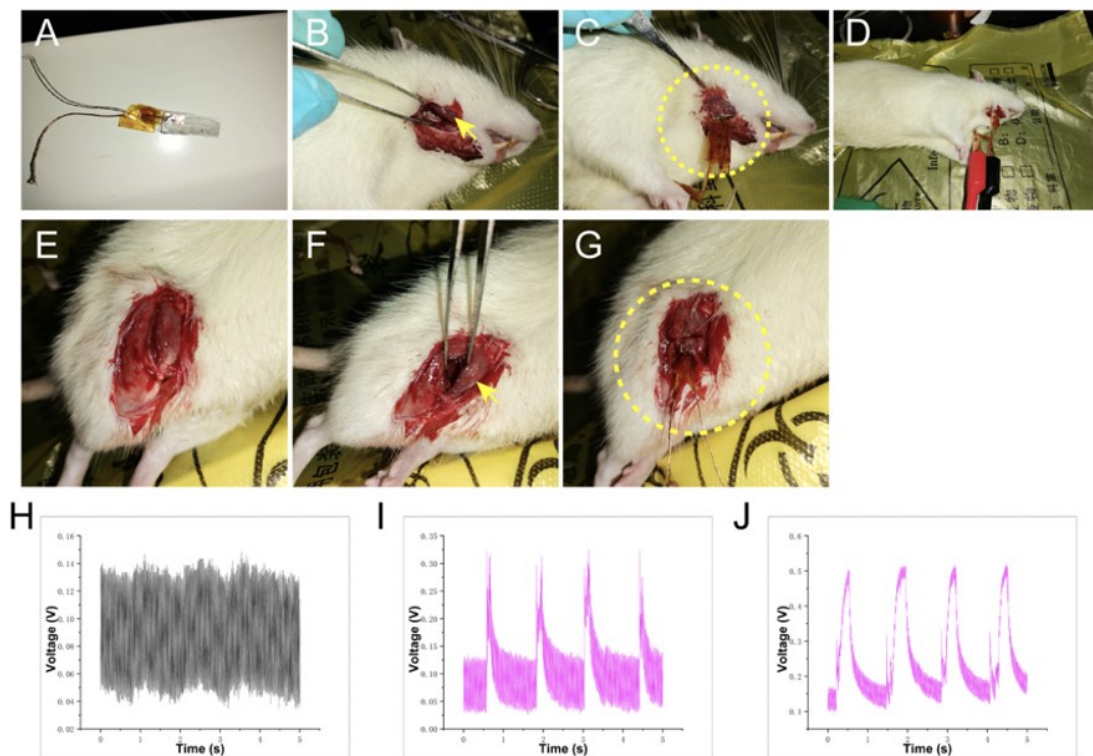


Fig. S8 In vivo measurement of piezoelectric properties of electrospinning nanofiber mats. (A) A simple piezoelectric nanogenerator (PENG) was produced. (B) Exposing the masseter (yellow arrow). (C) PENG was sutured to the medial surface of the masseter (dotted yellow circle). (D) Piezoelectric testing of open and closed mouths (a loaded of 100 M Ω). (E, F) Exposing the femoral muscle group (yellow arrow). (G) PENG was sutured to the medial side of the femoral muscle group (dotted yellow circle). (H) The voltage output of PCL mat sutured to the masseter, about 0.1v is triboelectricity (a loaded of 100 M Ω). (I) The ZnO/AVT mat stapled to the masseter produced a voltage output of approximately 0.32v (a loaded of 100 M Ω). (J) The ZnO/AVT mat stapled to the femoral muscle detected a voltage output of \sim 0.5v (a loaded of 100 M Ω).

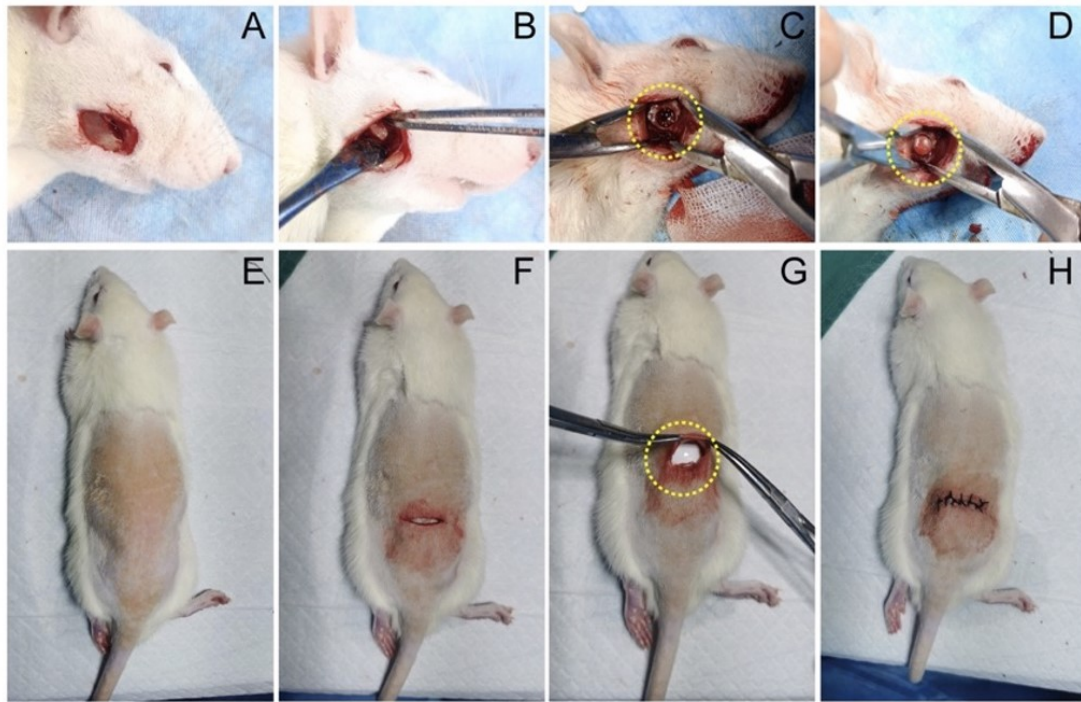


Fig. S9 Operative images of electrospun mat implantation for bone regeneration and angiogenesis in vivo. (A-D) After shaving and sterilization, a circular defect of 5 mm in diameter was prepared in the mandible and implanted with sterile electrospun mats. (E-H) After shaving and disinfection, sterile electrospun mats were implanted subcutaneously on the back of rats.

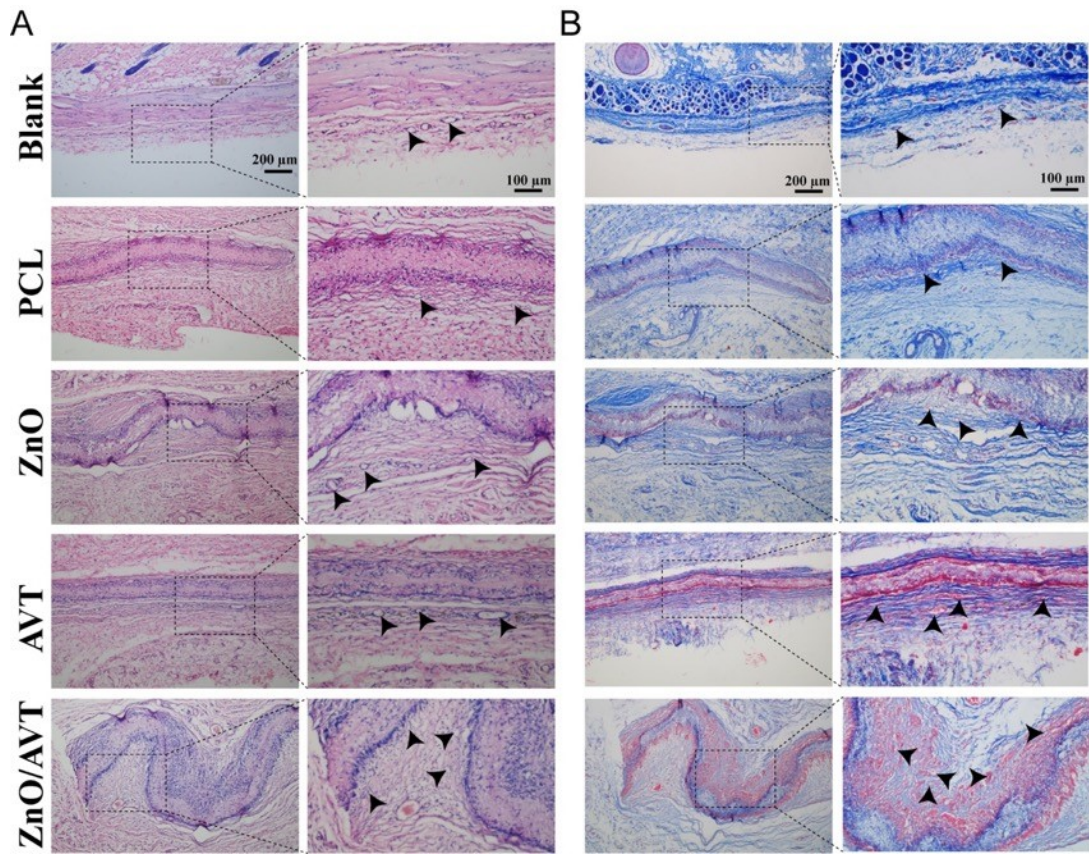


Fig. S10 Detection of the vasculogenic capacity of electrospun fiber mats in vivo. (A) HE staining of electrospun mats implanted subcutaneously for 4 weeks. (B) Masson staining of electrospun mats implanted subcutaneously for 4 weeks. Arrowheads indicate new blood vessels.

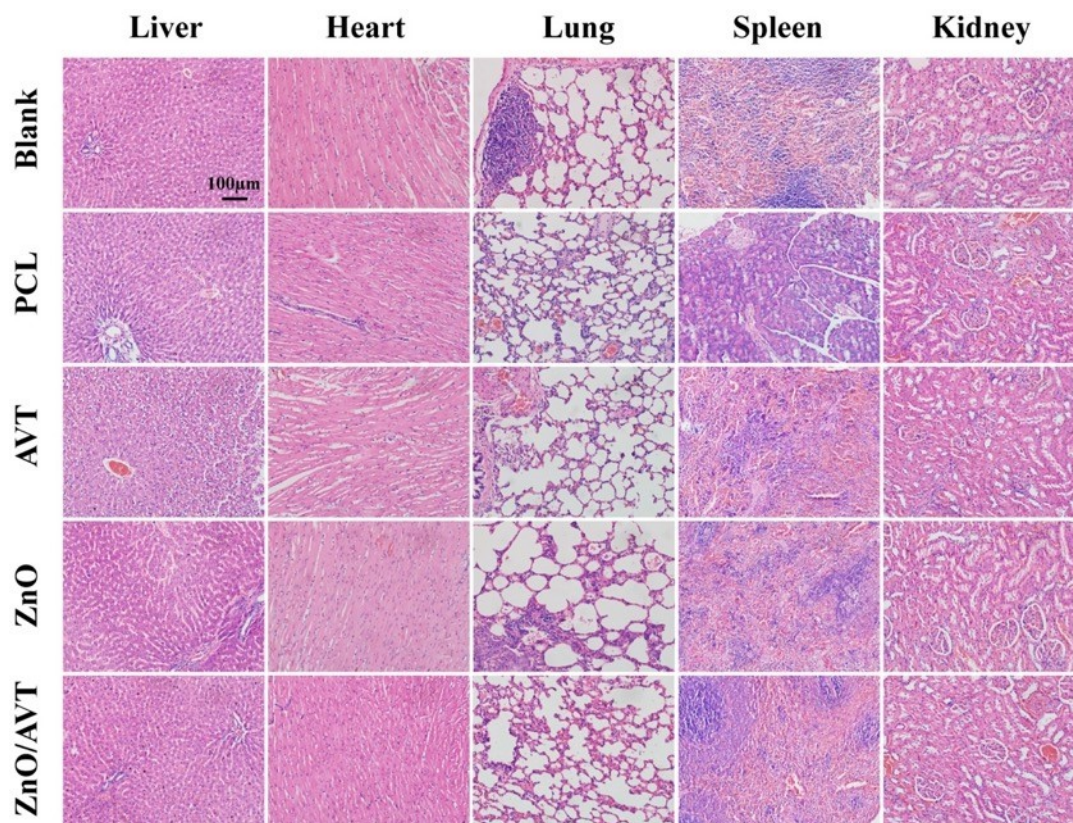


Fig. S11 HE staining of heart, liver, spleen, lungs, and kidneys 1 months after implantation of various electrospun mats showed excellent biocompatibility of mats loaded with different compositions.

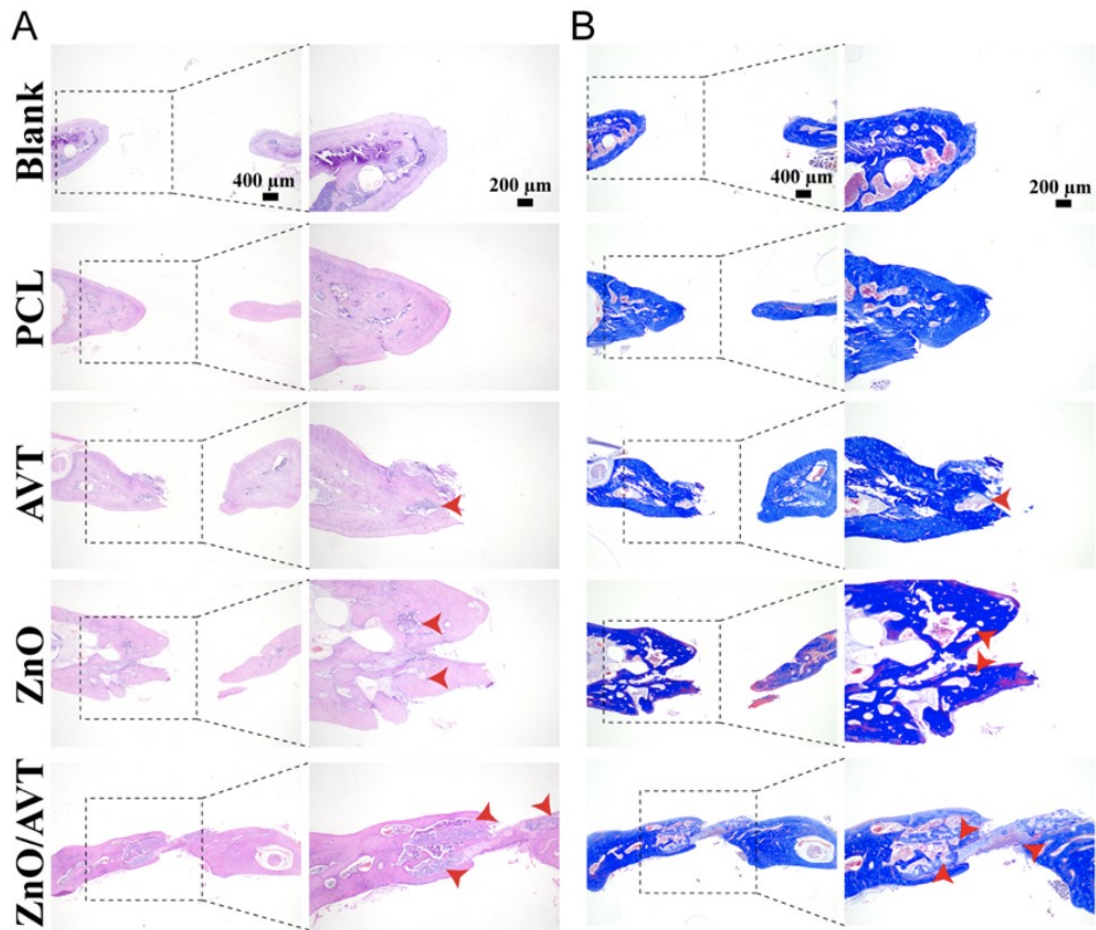


Fig. S12 Detection of the vasculogenic capacity of electrospun fiber mats in vivo. (A) HE staining of vascularized osteogenesis in mandibular defects 8 weeks after implantation. (B) Masson staining of vascularized osteogenesis in mandibular defects 8 weeks after implantation. Arrowheads indicate new blood vessels.

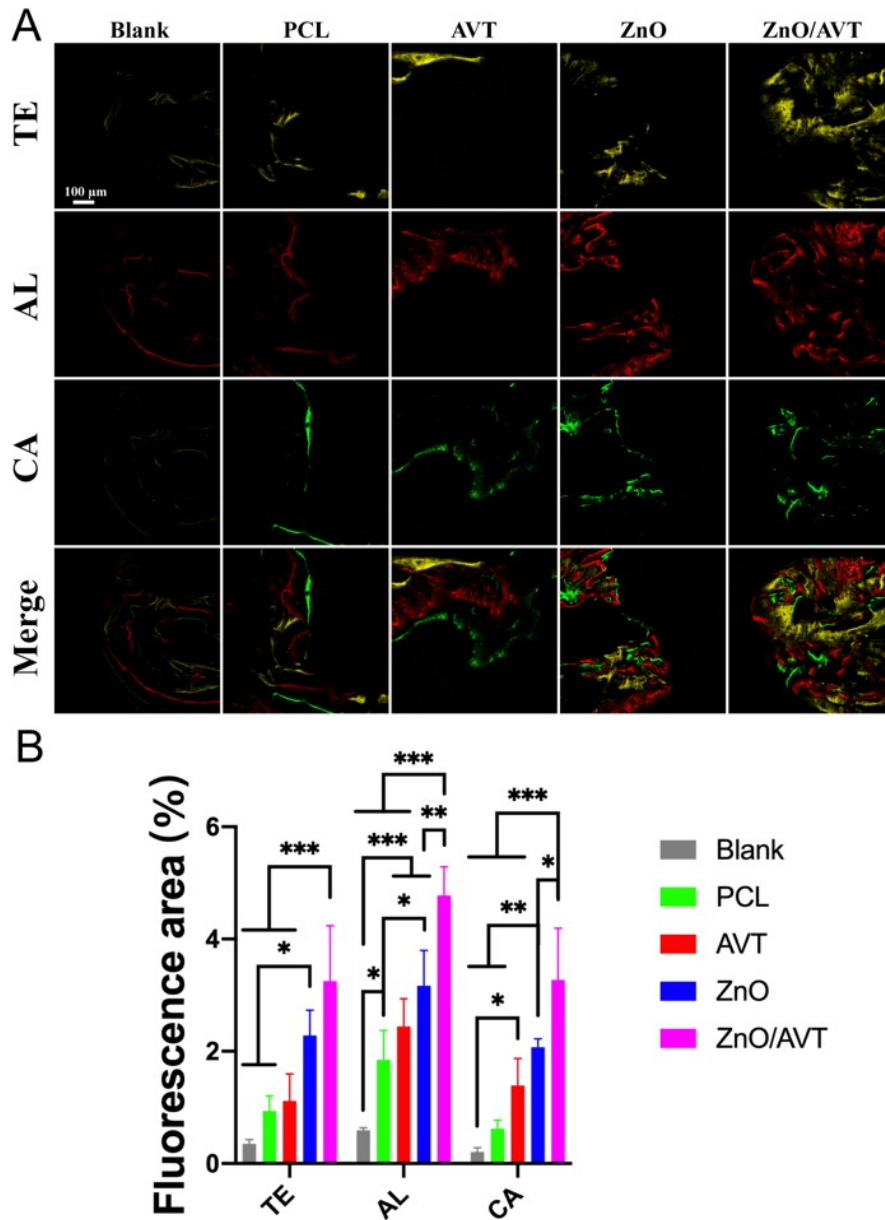


Fig.13 Sequential fluorescence staining of bone regeneration in mandibular defects. (A) CLSM images of sequential fluorescence-stained resin sections (New bone labeled with tetracycline (TE) for yellow fluorescence, alizarin red S (AL) for red fluorescence, and calcein (CE) for green fluorescence). (B) Quantitative analysis of fluorescence-stained bone regions. Data are expressed as mean \pm SD (n=4). The significance of data was calculated by one-way ANOVA (*represents $p < 0.05$, **represents $p < 0.01$, ***represents $p < 0.001$).

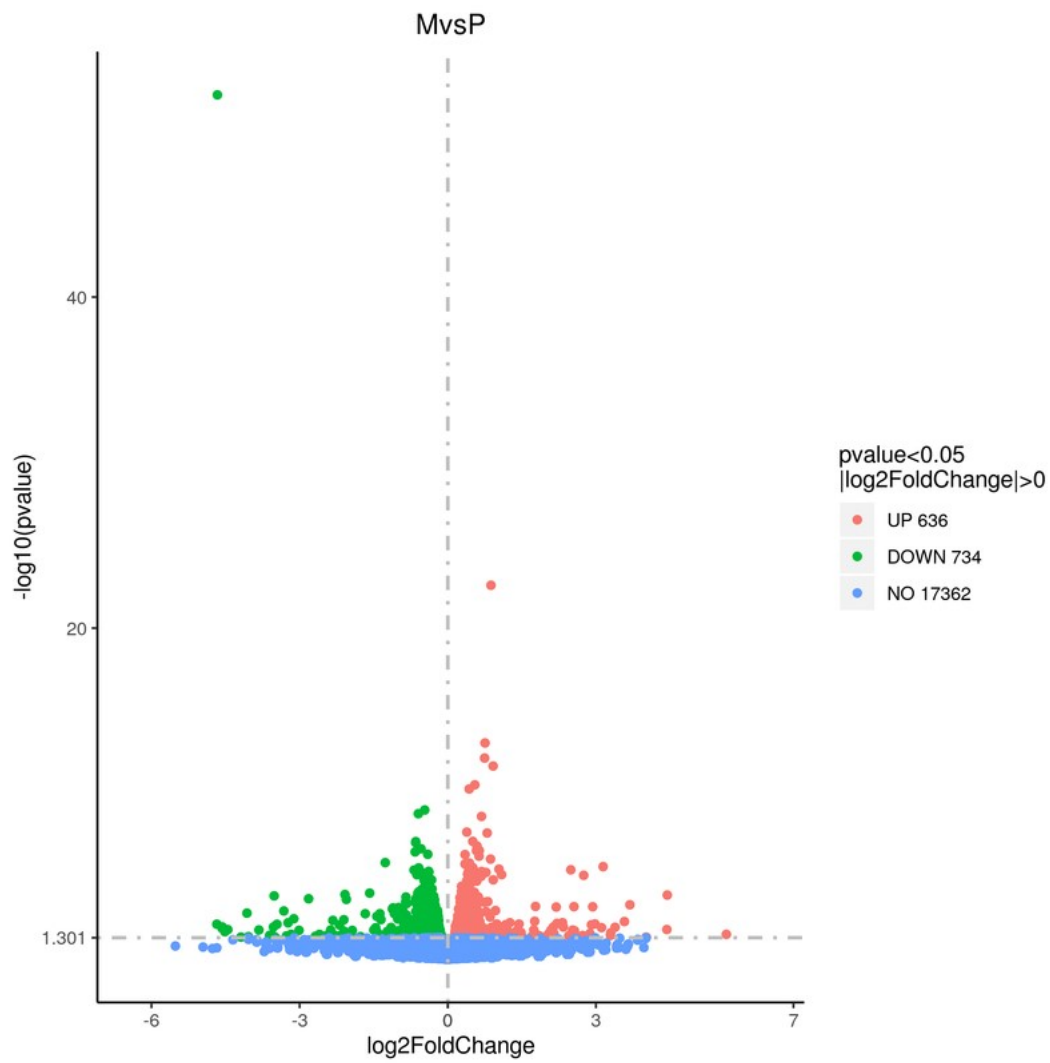


Fig. S14 Volcano maps of differential gene expression.

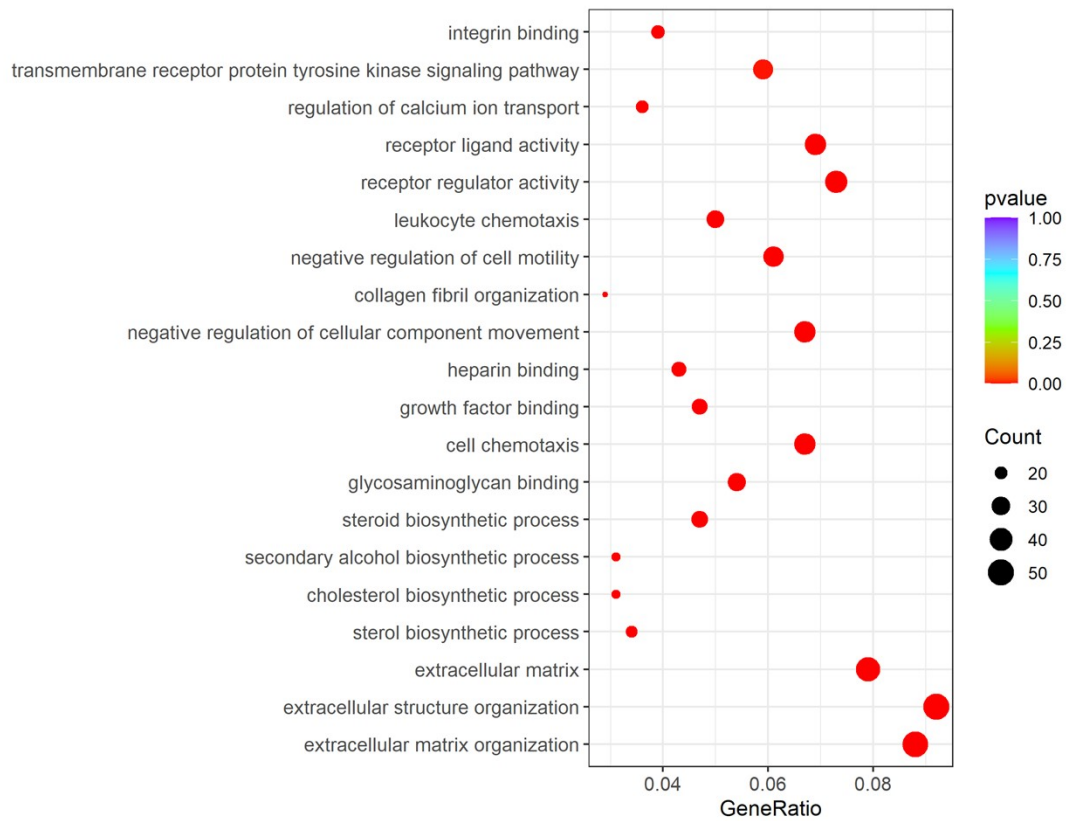


Fig. S15 20 significant gene ontology terms in the Biological Processes category of the ZnO/AVT mats relative to the PCL mats were shown as upregulated differentially expressed genes (DEGs).

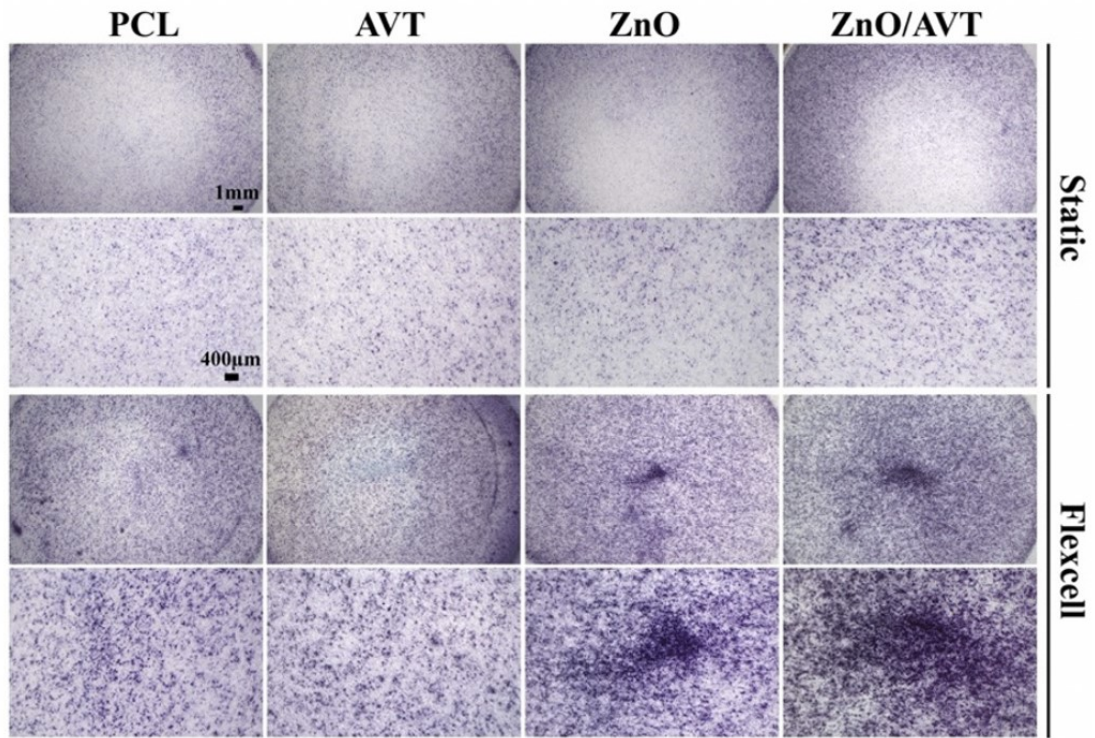
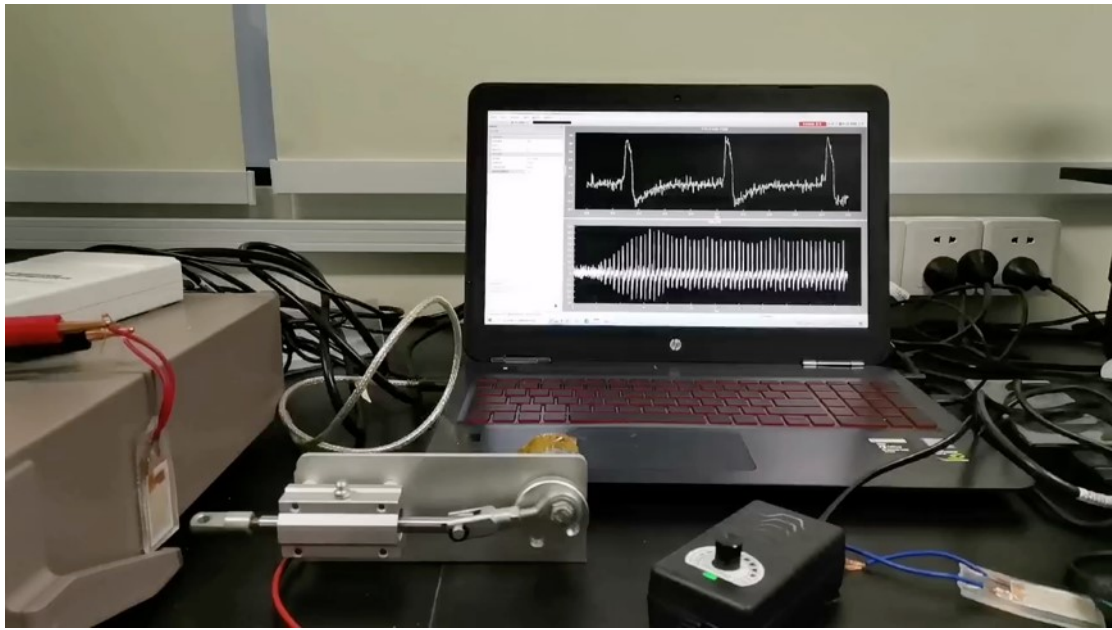
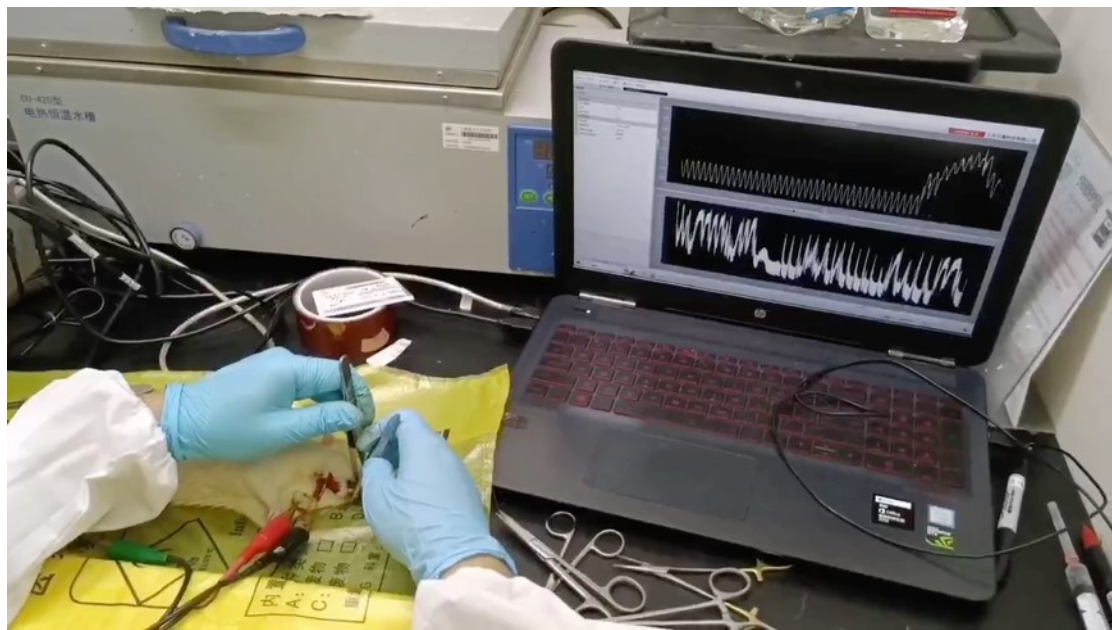


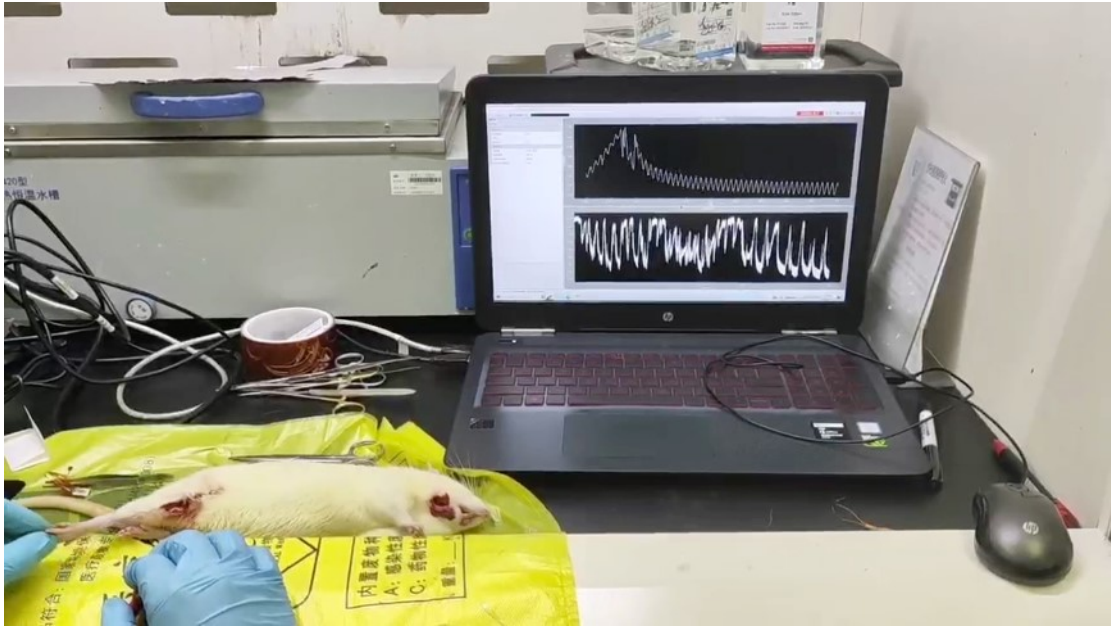
Fig. S16 Representative images of ALP staining of BMSCs cultured on different fiber mats for 7 days.



Video S1 Piezoelectric performance measurement of PENG.



Video S2 Piezoelectric output test of PENG on masseter.



Video S3 Piezoelectricity measurement of PENG on femoral muscle group.